

Spinodal decomposition via surface diffusion in polymer mixtures

J. Klein Wolterink,¹ G. T. Barkema,¹ and Sanjay Puri²

¹*Institute for Theoretical Physics, 3584 CE Utrecht, The Netherlands*

²*School of Physical Sciences, Jawaharlal Nehru University, New Delhi 110067, India*

(Received 11 January 2006; revised manuscript received 5 May 2006; published 20 July 2006)

We present experimental results for spinodal decomposition in polymer mixtures of gelatin and dextran. The domain growth law is found to be consistent with $t^{1/4}$ growth over extended time regimes. Similar results are obtained from lattice simulations of a polymer mixture. This slow growth arises due to the suppression of the bulk mobility of polymers. In that case, spinodal decomposition is driven by the diffusive transport of material along domain interfaces, which gives rise to a $t^{1/4}$ growth law.

DOI: [10.1103/PhysRevE.74.011804](https://doi.org/10.1103/PhysRevE.74.011804)

PACS number(s): 61.25.Hq

I. INTRODUCTION

A homogeneous binary mixture (AB) becomes thermodynamically unstable when it is quenched into the miscibility gap. The subsequent evolution of the mixture is characterized by the emergence and growth of domains enriched in either component [1–4]. This process of *domain growth* or *spinodal decomposition* is of great technological and scientific importance, and is relevant in diverse applications, e.g., the food-processing industry, metallurgy, materials science, etc. The standard experimental tools to characterize domain growth are (a) the time dependence of the typical domain size $\ell(t)$, and (b) the functional form of the structure factor, which depends on the system morphology. The domain growth law depends critically on the mechanism that drives phase separation. For example, diffusive transport of material through bulk domains yields the Lifshitz-Slyozov (LS) growth law $\ell(t) \sim t^{1/3}$, whereas diffusion along surfaces (interfaces) gives rise to a slower growth law $\ell(t) \sim t^{1/4}$ [5–8]. For binary fluid mixtures, the intermediate and late stages of phase separation are driven by the advective transport of material. The relevant growth laws (in $d=3$) are $\ell(t) \sim t$ in the *viscous hydrodynamic* regime, followed by $\ell(t) \sim t^{2/3}$ in the *inertial hydrodynamic* regime [1–4,9,10].

In the food processing industry, many applications involve domain growth in demixing polymer blends or quasi-binary polymer solutions (i.e., two kinds of polymers in a solvent). Polymeric phase separation has been studied experimentally in films of polymer blends [11–14], in thicker samples [15,16], and in dissolved mixtures [17]. The typical time scales of decomposition in these experiments vary from seconds [17] to days [16]. To characterize the speed of the coarsening process, one often fits a power law to the location of the maximum in the structure factor q_{\max} , as a function of time. Measurements of the resulting growth exponent α in $q_{\max} \sim t^{-\alpha}$ range from 0 to 0.45 [11,13,14]. Wiltzius and Cumming [15] report a value of $\alpha \approx 0.28$; Kuwahara *et al.* [16] report an evolution of this exponent from $\alpha \approx 0$ to $\alpha \approx 0.3$; and Takeno and Hashimoto [12] measure a value between 0.25 and 0.33. Clearly, there is no experimental consensus regarding the growth law. Moreover, the dominant mechanism for domain growth may differ in various experiments and time regimes, explaining the diverse exponents reported in the literature.

In this paper, we present results from an experimental and numerical study of spinodal decomposition in polymer mixtures in the high-viscosity regime (i.e., without hydrodynamics). This paper is organized as follows. In Sec. II, we present results from a light-scattering study of phase separation in a mixture of gelatin and dextran, dissolved in water. For deep quenches, domain growth in this system is consistent with the growth law $\ell(t) \sim t^{1/4}$ on the time scales of our experiment. In Sec. III, we present numerical results obtained from a lattice simulation of spinodal decomposition in a polymer mixture. Again, the domain growth law is found to be compatible with $\ell(t) \sim t^{1/4}$ over an extended time regime. In Sec. IV, we interpret these growth laws in the context of phase separation driven by surface diffusion, as the bulk mobility is drastically reduced in these polymer mixtures. Finally, Sec. V concludes this paper with a summary and discussion of our results.

II. EXPERIMENTAL DETAILS AND RESULTS

Let us first present details of the experiments. The chemicals used for our spinodal-decomposition experiments were gelatin (fish gelatin with a high molecular weight, Multi Products, lot 9187, box 47) and dextran (obtained from Sigma, industrial grade with an average molecular weight of 181 kg/mol, D-4876, lot 41K1243). These chemicals were used without further purification and dissolved in water. The concentration in the final sample for gelatin was 2.46 wt % and for dextran 2.40 wt %. No salt was added to the solution. However, azide was added to the stock solutions to halt bacterial growth. Earlier studies of phase separation in gelatin-dextran-water mixtures are due to Tromp *et al.* [18,19]. These authors investigated phase-separation morphologies and dynamical scaling for both shallow quenches (with temperatures $T > T_g$, the gelation temperature of gelatin) and deep quenches (with $T < T_g$). The light-scattering setup used by us is similar to that shown in Fig. 2 of Tromp *et al.* [18]. A He–Ne laser (633 nm) was used to generate a scattering pattern that was projected onto a screen of tracing paper. This is recorded by a charge-coupled device camera (EG&G PARC, Model 1430P). (See also Lundell *et al.* [20].) The usable q range was $0.3\text{--}7 \mu\text{m}^{-1}$.

The gelatin-dextran mixture described above is homogeneous at room temperature and starts to demix at a tempera-

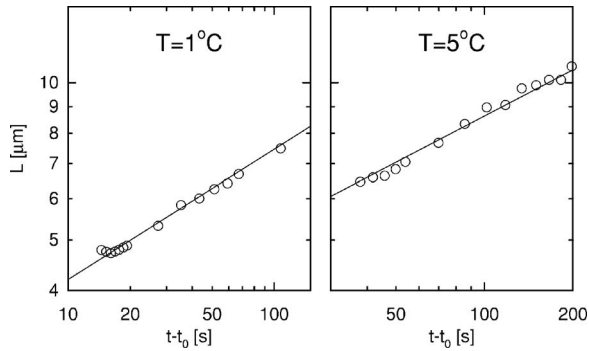


FIG. 1. Time dependence of length scale from experiments, plotted on a log-log scale. We study a deep quench to 1 °C (left frame) and a shallow quench to 5 °C (right frame). The lines denote the best linear fits to the experimental data. The corresponding growth exponents are $L \sim (t-t_0)^{0.25}$ (left) and $L \sim (t-t_0)^{0.29}$ (right).

ture ≈ 8 °C. The phase separation is clearly visible at 6 °C. This is close to the gelation temperature of the gelatin, which is estimated as 8–10 °C [21]. We specifically selected this mixture to obtain a high viscosity, so that hydrodynamic effects can be ignored on the time scales of our experiments.

Starting with a homogeneous mixture, we performed either a shallow quench to a final temperature of 5 °C, or a deep quench to 1 °C. From then on, the structure of the coarsening mixture is recorded at regular times with light scattering. Specifically, we obtain the typical domain size from $\ell(t) = 2\pi/q_{\max}(t)$, where $q_{\max}(t)$ is the location where the spherically averaged structure factor $S(q, t)$ reaches its maximum. For practical reasons, the time t_0 of the onset of phase separation is not known precisely in our experiments. We therefore determine t_0 from our measurements of $S(q, t)$ as follows. Assuming that the domain growth process is described by $q_{\max}(t) \sim (t-t_0)^{-\alpha}$ with $\alpha \approx 1/4$ or $1/3$, we perform a linear least-squares fit in which $q_{\max}^{-1/\alpha}$ is plotted vs t ; the time of zero crossing is then our estimate of t_0 . Since it takes some time before the structure factor develops a clear peak, we repeated this procedure also for the locations q'_{\max} and q''_{\max} of the maxima in $qS(q, t)$ and $q^2S(q, t)$. This results in six estimates for t_0 , which we average. We use the average value of t_0 to make a double-logarithmic plot of $\ell(t)$ vs $(t-t_0)$; the result is shown in Fig. 1.

As the straight lines in the figure indicate, domain growth after a deep quench to 1 °C is fitted well by $\ell(t) \sim (t-t_0)^{0.25}$, and after a shallow quench to 5 °C by $\ell(t) \sim (t-t_0)^{0.29}$. The deep quench convincingly shows a domain growth exponent in agreement with surface diffusion. There are two different scenarios for the reduction of bulk mobility in polymer mixtures (AB) at low temperatures. The first scenario is based on equilibrium properties. At the transition from the mixed to the demixed state, a delicate balance exists between the loss of entropy and the decrease in energy due to demixing. With increasing polymer length, both the entropy loss and the energetic decrease grow, and the transition becomes sharper with change in temperature. Thus, in polymer mixtures only a few degrees below the demixing temperature, the minority concentration (dextran in gelatin-rich domains and vice versa) is already negligible, ruling out

domain growth by bulk diffusion. The second scenario is based on dynamical properties. A single dextran (gelatin) molecule surrounded by gelatin (dextran) has the tendency to collapse onto itself. This has the effect that its mobility decreases, which in turn suppresses domain growth due to bulk diffusion. Both scenarios lead to the same conclusion: domain growth due to bulk diffusion is strongly suppressed in polymeric mixtures.

The shallow-quench experiment is not so conclusive. The larger growth exponent indicates that both surface and bulk diffusion contribute to coarsening, and we are in a crossover regime between $\alpha=1/4$ and $1/3$. The bulk mobility is enhanced at higher temperatures where A -rich bulk domains contain significant amounts of B , and vice versa. At this stage, it is relevant to make some general remarks about the crossover of growth exponents. Kendon *et al.* [22] have reported results from comprehensive lattice Boltzmann simulations of phase separation in low-viscosity fluids, where hydrodynamic effects are important. They find that the crossover from the viscous hydrodynamic regime to the inertial hydrodynamic regime is extremely slow and extends over several decades in time. As we will discuss later, the crossover from the surface-diffusion regime to the bulk-diffusion regime may also be highly extended. Therefore, one would need experimental (or numerical) data over several decades to clearly demarcate different growth regimes.

Our experiments are performed under conditions in which gelation takes place, so as to achieve a high viscosity and thereby suppress any hydrodynamic effects. An interesting issue is whether the gelation does more than only increasing the viscosity; does it suppress domain growth also in other ways? Since individual dextran molecules can still reptate through the gelatin, and since individual gelatin molecules are moving in an environment of dextran which does not gelate, there is no reason why domain growth through bulk diffusion would be suppressed as a direct consequence of gelation.

III. NUMERICAL DETAILS AND RESULTS

We have also performed extensive simulations of spinodal decomposition in a quasibinary polymer mixture. The specific model that we used is a lattice polymer model. Polymers with N bonds are described in this model as self-avoiding and mutually avoiding walks on a face-centered-cubic (fcc) lattice. The polymers move by a sequence of single-monomer jumps to nearest-neighbor lattice sites. For monomers that are neighbors along the same polymer, the steric interactions are lifted (and a site can thus be occupied by two or more adjacent monomers), as this allows enhanced reptation. A two-dimensional version of the model is illustrated in Fig. 2. This model is described in detail by Heukelum and Barkema [23].

Both reptation and Rouse dynamics are captured qualitatively in this model. Therefore, it can be used to study dynamical properties with some degree of realism, as long as hydrodynamic interactions are not essential. The main advantage of this model lies in its computational efficiency: elementary moves take only a few nanoseconds of CPU

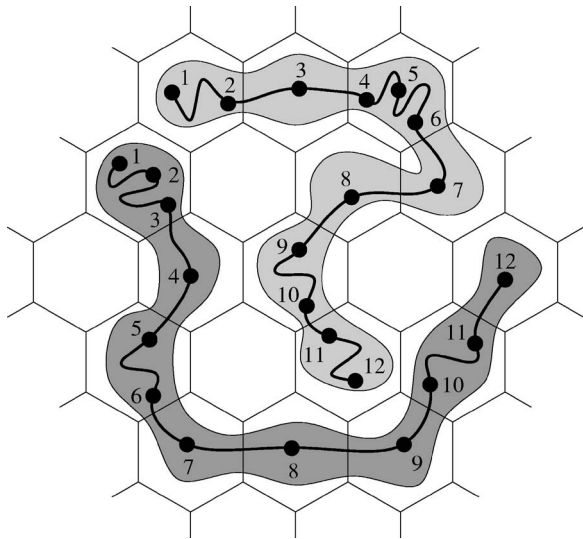


FIG. 2. Two-dimensional version of the lattice polymer model used in our simulations. In the upper polymer, interior monomers 2, 4, 6, 9, 10, and 11 can either diffuse along the tube or move sideways; monomer 7 can join either 6 or 8; the end monomers 1 and 12 can move to any vacant nearest-neighbor site. In the lower polymer, interior monomers 3, 5, 6, 10, and 11 can either diffuse along the tube or move sideways; monomer 1 can move to any vacant nearest-neighbor site, and monomer 12 can join its neighbor 11. All other monomers are immobile.

time, in contrast to microseconds in other polymer models. It has previously been used to study the fractionation of poly-dispersed polymer mixtures [24], diffusion and exchange of adsorbed polymers [25], desorption of polymers [26], and translocation of polymers through membranes [27].

The current study involves 128 000 polymers, each consisting of $N=50$ bonds and connecting 51 monomers. These are located on a three-dimensional fcc lattice with 8×10^6 sites and periodic boundary conditions. Half of the polymers are labeled as type *A* and the other half as type *B*. Polymers of different type repel each other: The total energy is equal to the number of pairs of neighboring sites occupied by different-type polymers, multiplied by an energy scale J . If an attempted Monte Carlo move increases the total energy by ΔE , the acceptance probability of this move is $P_a = \exp(-\beta\Delta E)$, where $\beta = 1/(k_B T)$ is the inverse temperature. Moves that do not raise the total energy are always accepted.

The simulations start from a mixed state, generated as an equilibrium configuration at high temperature ($\beta=0$). At $t=0$, the temperature is quenched to either $\beta J=0.05$ or $\beta J=0.1$. At these low temperatures, the repulsive *AB* interactions induce phase separation into domains rich in either *A* or *B*. The size of these domains grows in time—evolution snapshots for a typical run are shown in Fig. 3. To characterize domain growth, we assign to lattice site i occupied by an *A*-type (*B*-type) polymer the spin value $\sigma_i = +1$ (-1). The domain size is defined as the distance ℓ of the first zero crossing of the spatial correlation function of σ_i , and we measure it at various times. The time dependence of $\ell(t)$ is shown in Fig. 4 on a log-log scale. After an initial transient

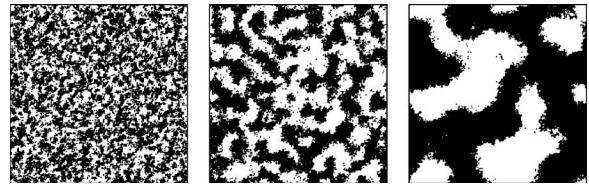


FIG. 3. Evolution pictures from simulations of spinodal decomposition in polymer mixtures. The details of the simulation are described in the text. The quench temperature was $\beta J=0.1$, and the system size is 200^3 . The pictures show a typical cross section of the three-dimensional lattice. The species *A* is marked in black, and the species *B* is not marked. The time in Monte Carlo steps (MCS) is, from left to right, $t=2776$, 160 065, and 9 230 100 MCS.

regime, both data sets (for $\beta J=0.05, 0.1$) are consistent with the growth law $\ell(t) \sim t^{1/4}$ over extended time regimes, viz., \sim two decades for $\beta J=0.05$ (denoted by circles), and ~ 2.5 decades for $\beta J=0.1$ (denoted by squares).

This growth law is consistent with phase separation via surface diffusion. The reduction in bulk mobility in our simulations is due to low-temperature dynamics. In the context of the Kawasaki spin-exchange model for phase separation, this can be understood by focusing on an interfacial pair with the minimum barrier for interchange: $\sigma_i = +1$ at the periphery of an up-rich domain and having only one neighbor with the same spin value, and $\sigma_j = -1$ in a down-rich domain. At low temperatures, the bulk domains are very pure and the energy barrier to the interchange $\sigma_i \leftrightarrow \sigma_j$ is qJ , where q is the number of nearest neighbors of a site. Thus, the time scale for this interchange $\tau_K \sim \exp(\beta\Delta\mathcal{H}) \rightarrow \infty$ as $T \rightarrow 0$, effectively blocking bulk diffusion. Of course, once an impurity spin is placed inside a bulk domain, there is no further barrier to its diffusion.

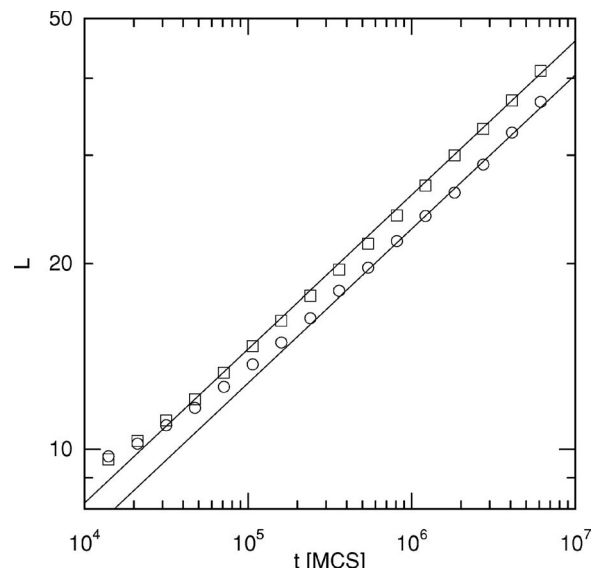


FIG. 4. Time dependence of length scale from simulations, plotted on a log-log scale. The time is measured in MCS. We show data for quenches to $\beta J=0.05$ (circles) and 0.1 (squares). The lines correspond to the growth law $\ell(t) \sim t^{1/4}$.

IV. GROWTH EXPONENTS DUE TO SURFACE AND BULK DIFFUSION

The above experimental and numerical results can be understood in the following theoretical framework [8]. The kinetics of diffusion-driven phase separation is described by the Cahn-Hilliard model [1–4]:

$$\frac{\partial}{\partial t} \psi(\vec{r}, t) = \vec{\nabla} \cdot \left[D(\psi) \vec{\nabla} \left(\frac{\delta F}{\delta \psi} \right) \right], \quad (1)$$

where $\psi(\vec{r}, t)$ is the order parameter at space point \vec{r} and time t . Typically, $\psi(\vec{r}, t) \approx \rho_A(\vec{r}, t) - \rho_B(\vec{r}, t)$, where ρ_A and ρ_B denote the local densities of species A and B . We have neglected thermal fluctuations in Eq. (1), and considered the general case of a ψ -dependent mobility $D(\psi)$ [28–30]. Further, $F[\psi]$ denotes the Helmholtz potential, which is usually taken to have the ψ^4 form: $F[\psi] \approx \int d\vec{r} [-\psi^2/2 + \psi^4/4 + (\vec{\nabla}\psi)^2/2]$, where we have used the order-parameter scale and the bulk correlation length to express $F[\psi]$ in dimensionless units. The A - and B -rich domains correspond to $\psi = +1$ and -1 , respectively.

Let us consider a situation where the mobility at the interfaces ($\psi = 0$) is D_s and that in the bulk ($\psi = \pm 1$) is D_b , with $D_b \leq D_s$. As stated earlier, this difference in interfacial and bulk mobilities can result from low-temperature dynamics, where there is a high-energy barrier for an A atom to enter a B -rich bulk domain and vice versa. Alternatively, physical processes like glass formation [31] or gelation [32,33] can also result in a drastic reduction in bulk mobility. A simple functional form for the mobility in the above case is $D(\psi) = D_s(1 - c\psi^2)$, where $c = 1 - D_b/D_s$. Notice that $0 \leq c \leq 1$ for $D_b \leq D_s$. Thus, Eq. (1) can be written as

$$\frac{\partial}{\partial t} \psi(\vec{r}, t) = \vec{\nabla} \cdot [(1 - c\psi^2) \vec{\nabla}(-\psi + \psi^3 - \nabla^2\psi)], \quad (2)$$

where we have absorbed D_s into the time scale.

Equation (2) can be decomposed as [6]

$$\begin{aligned} \frac{\partial}{\partial t} \psi(\vec{r}, t) = & (1 - c) \nabla^2(-\psi + \psi^3 - \nabla^2\psi) \\ & + c \vec{\nabla} \cdot [(1 - \psi^2) \vec{\nabla}(-\psi + \psi^3 - \nabla^2\psi)], \end{aligned} \quad (3)$$

where the first and second terms on the right-hand side correspond to bulk diffusion and surface diffusion, respectively. The bulk-diffusion term is absent in the limit $c = 1$ ($D_b = 0$). Further, the surface diffusion term is only relevant at interfaces, where $\psi = 0$. The location of the interfaces $\vec{r}_i(t)$ is defined by the zeros of the order-parameter field $\psi[\vec{r}_i(t), t] = 0$. Let us focus on a particular interface in the d -dimensional case. We denote the normal coordinate as n and the interfacial coordinates as \vec{a} . Then, the normal interface velocity $v_n(\vec{a}, t)$ obeys the equation [5,6]

$$\begin{aligned} 4 \int d\vec{a}' G[\vec{r}_i(\vec{a}), \vec{r}_i(\vec{a}')] v_n(\vec{a}', t) \\ \approx (1 - c) \sigma K(\vec{a}, t) + 4c \int d\vec{a}' G[\vec{r}_i(\vec{a}), \vec{r}_i(\vec{a}')] \nabla^2 K(\vec{a}', t). \end{aligned} \quad (4)$$

Here, $K(\vec{a}, t)$ is the local curvature at point \vec{a} on the interface, and σ is the surface tension. The Green's function $G(\vec{x}, \vec{x}')$ is obtained from $-\nabla^2 G(\vec{x}, \vec{x}') = \delta(\vec{x} - \vec{x}')$.

A dimensional analysis of Eq. (4) yields the growth laws due to surface and bulk diffusion. The scales of various quantities are as follows: $[d\vec{a}] \sim \ell^{d-1}$, $[G] \sim \ell^{2-d}$, $[v_n] \sim d\ell/dt$, $[K] \sim \ell^{-1}$. This yields the crossover behavior of the length scale as

$$\ell(t) \sim \begin{cases} (ct)^{1/4}, & t \ll t_c, \\ [(1 - c)\sigma t]^{1/3}, & t \gg t_c, \end{cases} \quad (5)$$

where $t_c \sim c^3 / [(1 - c)^4 \sigma^4]$. Notice that the asymptotic regime obeys the LS growth law, which is characteristic of growth driven by bulk diffusion. However, the crossover to the LS regime can be strongly delayed if the bulk mobility is suppressed relative to the surface mobility, i.e., $D_b/D_s \rightarrow 0$ or $c \rightarrow 1$. Note that the mobility of individual dextran (gelatin) molecules in a dextran- (gelatin-) rich environment does not lead to domain growth.

V. SUMMARY AND DISCUSSION

Let us conclude this paper by summarizing the results presented here. First, we presented results from light-scattering studies of phase-separation kinetics in gelatin-dextran-water mixtures. We can neglect hydrodynamic effects in these mixtures as the fluid velocity field is rapidly dissipated due to high viscosity. Therefore, domain growth is driven by the diffusive transport of material. For deep quenches, the domain growth law is compatible with $\ell(t) \sim t^{1/4}$ over an extended time regime. This slower growth arises because there is a strong suppression of mobility of the minority species in the bulk domains of the other species. Therefore, domain growth is primarily driven by diffusive transport along interfacial regions, which gives rise to a $t^{1/4}$ -growth law.

Second, we presented results from a large-scale simulation of spinodal decomposition in a quasibinary polymer mixture. Again, domain growth in this system is compatible with phase separation driven by surface diffusion. Understanding the mechanism of demixing not only is important for identifying the domain growth exponent, it is also a prerequisite for obtaining control over the structure formation. We hope that the results presented here will stimulate further experimental and numerical interest in this problem.

ACKNOWLEDGMENTS

We would like to thank Hans Tromp from NIZO food research for his kind hospitality, and Arjan Visser for preliminary simulations.

- [1] A. J. Bray, *Adv. Phys.* **43**, 357 (1994).
- [2] K. Binder and P. Fratzl, in *Phase Transformations in Materials*, edited by G. Kostorz (Wiley-VCH, Weinheim, 2001), p. 409.
- [3] A. Onuki, *Phase Transition Dynamics* (Cambridge University Press, Cambridge, U.K., 2002).
- [4] S. Dattagupta and S. Puri, *Dissipative Phenomena in Condensed Matter: Some Applications* (Springer-Verlag, Heidelberg, 2004).
- [5] T. Ohta, *J. Phys. C* **21**, L361 (1988); K. Kawasaki and T. Ohta, *Prog. Theor. Phys.* **68**, 129 (1982).
- [6] A. M. Lacasta, A. Hernandez-Machado, J. M. Sancho, and R. Toral, *Phys. Rev. B* **45**, 5276 (1992); A. M. Lacasta, J. M. Sancho, A. Hernandez-Machado, and R. Toral, *ibid.* **48**, 6854 (1993).
- [7] S. Puri, A. J. Bray, and J. L. Lebowitz, *Phys. Rev. E* **56**, 758 (1997).
- [8] S. van Gemmert, G. T. Barkema, and S. Puri, *Phys. Rev. E* **72**, 046131 (2005).
- [9] T. Koga and K. Kawasaki, *Phys. Rev. A* **44**, R817 (1991).
- [10] S. Puri and B. Dunweg, *Phys. Rev. A* **45**, R6977 (1992).
- [11] J. Lauger, R. Lay, and W. Gronski, *J. Chem. Phys.* **101**, 7181 (1994).
- [12] H. Takeno and T. Hashimoto, *J. Chem. Phys.* **108**, 1225 (1998).
- [13] M. Hayashi, H. Jinnai, and T. Hashimoto, *J. Chem. Phys.* **113**, 7554 (2000).
- [14] M. Hayashi, H. Jinnai, and T. Hashimoto, *J. Chem. Phys.* **112**, 6886 (2000); **112**, 6897 (2000).
- [15] P. Wiltzius and A. Cumming, *Phys. Rev. Lett.* **66**, 3000 (1991).
- [16] N. Kuwahara, H. Sato, and K. Kubota, *J. Chem. Phys.* **97**, 5905 (1992).
- [17] B. Steinhoff, M. Rullmann, L. Kuhne, and I. Alig, *J. Chem. Phys.* **107**, 5217 (1997).
- [18] R. H. Tromp, A. R. Rennie, and R. A. L. Jones, *Macromolecules* **28**, 4129 (1995).
- [19] R. H. Tromp and R. A. L. Jones, *Macromolecules* **29**, 8109 (1996).
- [20] C. Lundell, E. H. A. de Hoog, R. H. Tromp, and A. M. Hermansson, *J. Colloid Interface Sci.* **288**, 222 (2005).
- [21] R. H. Tromp, E. ten Grotenhuis, and C. Olieman, *Food Hydrocolloids* **16**, 235 (2002).
- [22] V. M. Kendon, J.-C. Desplat, P. Bladon, and M. E. Cates, *Phys. Rev. Lett.* **83**, 576 (1999); V. M. Kendon, M. E. Cates, I. Pagonabarraga, J.-C. Desplat, and P. Bladon, *J. Fluid Mech.* **440**, 147 (2001).
- [23] A. van Heukelum and G. T. Barkema, *J. Chem. Phys.* **119**, 8197 (2003).
- [24] A. van Heukelum, G. T. Barkema, M. W. Edelman, E. van der Linden, E. H. A. de Hoog, and R. H. Tromp, *Macromolecules* **36**, 6662 (2003).
- [25] J. Klein Wolterink, G. T. Barkema, and M. A. Cohen Stuart, *Macromolecules* **38**, 2009 (2005).
- [26] J. Klein Wolterink, M. A. Cohen Stuart, and G. T. Barkema, *Mol. Phys.* **104**, 639 (2006).
- [27] J. Klein Wolterink, G. T. Barkema, and D. Panja, *Phys. Rev. Lett.* **96**, 208301 (2006).
- [28] J. S. Langer, M. Bar-on, and H. D. Miller, *Phys. Rev. A* **11**, 1417 (1975).
- [29] K. Kitahara and M. Imada, *Suppl. Prog. Theor. Phys.* **64**, 65 (1978); K. Kitahara, Y. Oono, and D. Jasnow, *Mod. Phys. Lett. B* **2**, 765 (1988).
- [30] S. Puri, K. Binder, and S. Dattagupta, *Phys. Rev. B* **46**, 98 (1992); S. Puri, N. Parekh, and S. Dattagupta, *J. Stat. Phys.* **77**, 839 (1994).
- [31] D. Sappelt and J. Jackle, *Europhys. Lett.* **37**, 13 (1997); *Polymer* **39**, 5253 (1998).
- [32] F. Sciortino, R. Bansil, H. E. Stanley, and P. Alstrom, *Phys. Rev. E* **47**, 4615 (1993).
- [33] J. Sharma and S. Puri, *Phys. Rev. E* **64**, 021513 (2001); A. Onuki and S. Puri, *ibid.* **59**, R1331 (1999).